Russian Physics Journal, Vol. 56, No. 5, October, 2013 (Russian Original No. 5, May, 2013)

DYNAMIC MODEL OF THE FORMATION OF AN INTERMEDIATE MESORCOPIC STATE DURING *B*2 → *B*19 MARTENSITIC TRANSFORMATION

M. P. Kashchenko[1,2] and V. G. Chashchina[1,2]

UDC 669.018.2

Morphological characteristics of martensite after B2–B19 transformation are considered within the limits of the concept of the control wave process. It is demonstrated that there is a possibility for the fast formation of an intermediate mesoscopic state. The instability of this state for the subsequent transition to final strains is supposed.

Keywords: dynamic theory, martensitic transformations, titanium nickelide, morphological characteristics.

INTRODUCTION

Progress in the development of the dynamic theory of reconstructive martensitic transformations (MT) [1–5] is based on a new paradigm, additional to the traditional scheme of equilibrium thermodynamics. The key role here is played by the concept of the initial excited state (IES) appearing in the elastic field of a dislocation nucleation center (DNC). The oscillatory character of the IES generates a control wave process (CWP) resulting in the threshold deformation disruption of the stability of the initial phase. Synthesis of concepts of heterogeneous nucleation and wave growth is reached if we consider that the wave normals $\boldsymbol{n}_1$ and $\boldsymbol{n}_2$ of wave beams in the CWP, describing in the superposition region the tensile ($\varepsilon_1 > 0$) or compression strain ($\varepsilon_2 < 0$), are collinear to the eigenvectors ξ_i (i = 1, 2) of the strain tensor of the elastic defect field in the nucleation region:

$$\boldsymbol{n}_1 \| \xi_1, \boldsymbol{n}_2 \| \xi_2, \boldsymbol{n}_1 \perp \boldsymbol{n}_2, |\boldsymbol{n}_1| = |\xi_i| = 1. \tag{1}$$

The normal $\boldsymbol{N}_\text{w}$ to the habit plane associated with CWP propagation is set by the relationship

$$\boldsymbol{N}_\text{w} \| \boldsymbol{n_2} - \boldsymbol{n_1}æ, \; æ = \frac{v_2}{v_1}, \tag{2}$$

where v_1 and v_2 are moduli of the velocities of wave propagation in $\boldsymbol{n}_1$ and $\boldsymbol{n}_2$ directions. For small threshold strains ε_th, the relationship

$$æ = \frac{v_2}{v_1} \; k \approx \sqrt{\frac{\varepsilon_1}{|\varepsilon_2|}} \tag{3}$$

holds true. The reconstructive MT possess clearly pronounced properties of cooperative phase transitions of the first kind, whereas in the *B*2 titanium–nickelide-based alloys, the characteristics of transitions of the first kind are expressed to a lesser degree. From three widespread MT variants (*B*2 → *B*19, *B*2 → *R*, and *B*2 → *B*19′), we consider here the

[1]Ural State Forest Engineering University, Ekaterinburg, Russia; [2]Ural Federal University Named after the First President of Russia B. N. El'tsin, Ekaterinburg, Russia, e-mail: mpk46@mail.ru. Translated from Izvestiya Vysshikh Uchebnykh Zavedenii, Fizika, No. 5, pp. 65–68, May, 2013. Original article submitted April 10, 2013.

$B2 \rightarrow B19$ transition with the greatest relative change of the volume. Attention is focused on CWP cases [4–6] providing the fastest transformation of the $\{110\}_{B2}$ planes. The present work is aimed at demonstration of the possibility of a choice of the deformable plane convenient for a description of the $B2 \rightarrow B19$ (and $B2 \rightarrow B19'$) MT through the intermediate mesoscopic state.

EXPECTED HABIT PLANES AND DNC FOR QUENCHED MARTENSITE CRYSTALS

Based on the data on the elastic moduli of Ti–Ni–Cu and Ti_{50}–Ni_{38}–Cu_{10}–Fe_2 systems presented in [7–9, 10], the elastic moduli (in GPa) are assumed to be

$$C_{11} = 165,\ C_{12} = 139,\ C_{44} = 34. \tag{4}$$

Setting in Eq. (2) $\boldsymbol{n}_1 \| [110]_{B2}$ and $\boldsymbol{n}_2 \| [001]_{B2}$ (the $(1\ \bar{1}\ 0)_{B2}$ plane is deformed), we find

$$\boldsymbol{N}_w \| [\ \bar{æ}\bar{æ}\ \sqrt{2}\ ]_{B2},\ æ = \sqrt{\frac{2\,C_{11}}{C_{11} + C_{12} + 2\,C_{44}}}\ . \tag{5}$$

Substitution of elastic moduli (4) into Eq. (5) yields

$$æ \approx 0.9419 \text{ and } \boldsymbol{N}_w \| \left[\bar{1}\ \ \bar{1}\ \ 1.5015\right]_{B2}, \tag{6}$$

that is, the $\{223\}_{B2}$ habit planes, as well as $\{334\}_{B2}$ ones (for small deviations of $\boldsymbol{n}_1$ and $\boldsymbol{n}_2$ from the symmetry axes), are easily realized in the wave description. It is well known (for example, see [11, 12]) that the necessary conditions for the formation of the corresponding IES exist in elastic fields of edge dislocations with $\left[1\ \bar{1}\ 0\right]_{B2}$ lines. Recall that the habit planes, close to $\{223\}_{B2}$ and $\{334\}_{B2}$, are observed in Ti–Ni–Cu [13].

RATIO OF STRAINS

The $B19$ phase is orthorhombic; therefore, the additional requirement caused by the lattice symmetry during α–ε MT (see [5]) is absent, and it is impossible to determine analytically the final strains from their well-known ratio. However, knowing the lattice parameters for the initial and final phases, it is possible to verify whether the observable ratio of final strains is in agreement with its value according to requirement (3). Figure 1 taken from [7] shows elementary cells of phases.

It should be borne in mind that Fig. 1 displays only approximate correspondence of cell sizes of the initial $B2$ phase. For example, setting the cell size in the $[100]_{B2}$ direction equal to $a_{B2} = 0.3$ nm, the sizes in the $[011]_{B2}$ and $[01\bar{1}]_{B2}$ directions must be set equal to $\sqrt{2}\,a_{B2} \approx 0.42426$ nm rather than 0.43 nm. Below it is expedient to take advantage of experimental data for the lattice parameters with greater number of significant digits. Thus, according to [13], we have

$$a_{B2} = 0.3030 \text{ nm},\ a_{B19} = 0.2881 \text{ nm},\ b_{B19} = 0.4279 \text{ nm},\ c_{B19} = 0.4514 \text{ nm}. \tag{7}$$

A comparison of data (7) with data in Fig. 1 demonstrates the maximum difference between values of the parameter b_{B19}.

From Fig. 1 it is clear that the final strains of the $B2$ phase cell are determined by formulas

$$\varepsilon_{[100]} = (a_{B19} - a_{B2})/a_{B2},\ \varepsilon_{[01\bar{1}]} = (b_{B19} - \sqrt{2}\,a_{B2}) / (\sqrt{2}\,a_{B2}),\ \varepsilon_{[011]} = (c_{B19} - \sqrt{2}\,a_{B2}) / (\sqrt{2}\,a_{B2}). \tag{8}$$

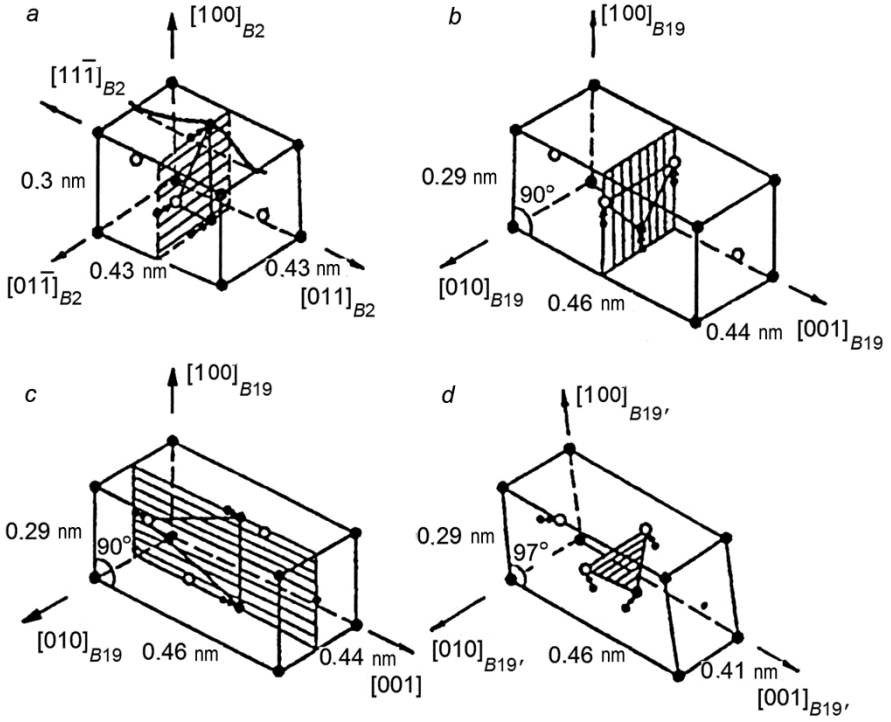

Fig. 1. Elementary cells of *B*2 (*a*), *B*19 (*b* and *c*), and *B*19′ phases (*d*) in titanium nickelide alloys and their size-orientation relations and transformation schemes determined by shuffle ({011}<100> and $\{01\bar{1}\}$<011> type) displacements of atoms (the $\{011\}_{B2}$ shear planes are hatched). The figure corresponds to Fig. 3.12 in [7].

From Eq. (8) with values of the parameters given by Eq. (7) we obtain

$$\varepsilon_{[100]} \approx -0.04917,\ \varepsilon_{[01\bar{1}]} \approx -0.00142,\ \varepsilon_{[011]} \approx 0.05343. \tag{9}$$

Since the strain $\varepsilon_{[01\bar{1}]} \approx -0.00142$ in Eq. (9) is 10 times less than two others, it is obvious that the plane $(01\bar{1})_{B2}$ experiences the fastest tensile-compressive strain in the orthogonal $[100]_{B2}$ and $[011]_{B2}$ directions. Choosing $\varepsilon_{[011]} \approx 0.05343$ for ε_1 and $\varepsilon_{[100]} \approx -0.04917$ for ε_2, we obtain the ratio of strains

$$\varepsilon_1 / |\varepsilon_2| \approx 1.0865. \tag{10}$$

From Eq. (6) we obtain $æ^2 \approx 0.8872$. According to Eq. (10), $\varepsilon_1 / |\varepsilon_2| > 1$ and $æ^2 < 1$; therefore, the ratio of the final strains deviates from that set by condition (3) in the threshold regime.

We note that the fulfillment of condition (3) would mean smaller tensile strain value in comparison with the compressive strain for a pair of relatively long-wavelength beams (ℓ-beams), responsible for the formation of the habit plane of a martensite crystal. Analogous situation is observed during γ−α MT in iron-based alloys. Moreover, by analogy with [14, 15], it is clear that in the presence in the CWP structure of relatively short-wavelength displacements (*s*-beams) responsible for the formation of the main component of transformation twins (with alternating principal tension axes), condition (3) can be met for ℓ-beams up to the final strains for *B*2–*B*19 MT as well.

However, *B*19 martensite, as a rule, is not twinned. In this case, in our opinion, another transformation scenario not discussed earlier can be observed.

HYPOTHESIS ABOUT THE INTERMEDIATE MESOSCALE STATE

Since the strain rate of $B19$ martensite crystals is high and the observed habit planes are easily described by the wave model, it is possible to assume that actually, the CWP induces the first (main) stage of the fastest strain of the $(01\bar{1})_{B2}$ plane. In this stage, the final compression strain ε_2 and the intermediate value of the tensile strain ε_1 are attained. The subsequent stage is associated with additional (rather small) stretching in the $[011]_{B2}$ direction caused, most likely, by electron correlations. Then the CWP will determine the parameters a_{B19} and c'_{B19} according to the condition $\varepsilon_1/|\varepsilon_2| \approx æ^2$. For example, for $|\varepsilon_2| = 0.04917$ and $æ^2 = 0.8872$, we obtain $\varepsilon_1 \approx 0.04362$, that is, the strain $\varepsilon_1 \approx 0.01$ is retained for the second stage. The lattice parameter c'_{B19} is $\sqrt{2}\,a_{B2}(1 + \varepsilon_1) \approx 0.4472$ nm. This sequence of transformations is also suitable for a description of the $B2 \rightarrow B19'$ transformation. Indeed, it is convenient to consider the fast formed (due to CWP stimulation) state, after compression strain ε_2 along $[100]_{B2}$ and tensile strain $\varepsilon_1 = (c'_{B19} - \sqrt{2}\,a_{B2})/(\sqrt{2}\,a_{B2})$ along $[011]_{B2}$, as an unstable intermediate mesoscale state (IMS). The IMS $\rightarrow B19$ transition is accompanied by additional stretching in the $[011]_{B2}$ direction (and possibly by a smaller strain in the $[01\bar{1}]_{B2}$ direction). The IMS $\rightarrow B19'$ transition is associated with the coordinated tension along $[011]_{B2}$ and compression along $[01\bar{1}]_{B2}$. We note that tensile and compressive strains for the IMS $\rightarrow B19'$ transition are approximately equal. This means that the IMS $\rightarrow B19'$ transition can proceed in the wave mode for which condition (3) holds true, because the velocities of waves in the equivalent directions are identical and hence $æ = 1$.

ORIENTATION RELATIONSHIPS

First of all, proceeding to orientation relationships (OR) for the IMS, we note that for the fastest transformation of a plane, for example, $(011)_{B2}$, it is possible to expect that this plane will enter into OR:

$$(011)_{B2} \parallel (001)_{B19}, \tag{11}$$

and the given plane will be orthogonal to the habit one. According to [5, 14, 15], one of the variants of recording the analytical dependence of the misorientation angle φ for the corresponding directions on the wave velocity ratio æ has the form

$$\varphi(æ) = \arccos \frac{\Gamma + æ^2}{\sqrt{(\Gamma^2 + æ^2)(æ^2 + 1)}},\ \Gamma = \frac{1 + \varepsilon_1}{1 - |\varepsilon_2|}. \tag{12}$$

In the case of the $B2$–IMS transition, the replacement $\varepsilon_1 \rightarrow \varepsilon_2$ in Eq. (12) should be borne in mind. In the examined case, the angle $\varphi(æ)$ describes rotation of the $<100>_{B2}$, $<01\bar{1}>_{B2}$ reference point about the $<011>_{B2}$ axis. Substituting in Eq. (12) $æ^2 \approx 0.8872$, $\varepsilon_1 \approx 0.04362$, $|\varepsilon_2| = 0.04917$, and $\Gamma \approx 1.0976$, we obtain $\varphi(æ) \approx 2.6516°$.

Additional strain during IMS–$B2$ and IMS–$B19$ rearrangements leads to an increase in $\varphi(æ)$ within the limits of 3°. It should be noted that the Bain variant of the orientation relations equivalent to the special case of OR (11) and (12) at $\varphi = 0$ was indicated in [7] as the OR for the $B2 \rightarrow B19'$ and $B2 \rightarrow B19$ transformations. Our estimate of the OR demonstrates that the OR must be determined as exact as possible to judge the mechanism of cooperative transformation. In our opinion, the exact fulfillment of the Bain OR would demonstrate that the conditions for material rotation of the lattice were not met in experiments with foils under examined conditions. In the general case, OR (11) and (12) are preferable.

CONCLUSIONS

Our analysis has demonstrated that the two-stage variant of implementation of the $B19$ phase in crystals is possible. The first stage is associated with the fastest strain of one of the family of planes $\{110\}_{B2}$ with incomplete

tensile strain attained in the second stage. In essence, the first stage leads to the fast formation of the intermediate mesoscopic state in which two lattice parameters differ from their final values. It is not excluded that the $B2 \rightarrow \text{IMS} \rightarrow B19$ transformation is competitive with the direct channel $B2 \rightarrow B19$, and the sequence $B2 \rightarrow \text{IMS} \rightarrow B19'$ is even preferable compared to the channel $B2 \rightarrow B19 \rightarrow B19'$.

This work was supported in part by the Russian Foundation for Basic Research (Project No. 11-08-96020).

REFERENCES

1. M. P. Kashchenko and V. G. Chashchina, Usp. Fiz. Nauk, **181**, No. 4, 345–364 (2011).
2. M. P. Kashchenko and V. G. Chashchina, Mater. Sci. Forum, **738–739**, 3–9 (2013).
3. M. P. Kashchenko, Wave Model of Martensite Growth during γ–α Transformation in Iron-Based Alloys [in Russian], Scientific and Publishing Center "Regular and Chaotic Dynamics," Izhevsk Institute of Computer Science, Moscow–Izhevsk (2010).
4. M. P. Kashchenko and V. G. Chashchina, Fiz. Met. Metalloved., **105**, No. 6, 571–577 (2008).
5. M. P. Kashchenko and V. G. Chashchina, Fiz. Met. Metalloved., **106**, No. 1, 16–25 (2008).
6. V. G. Chashchina, Russ. Phys. J., **52**, No. 7, 766–769 (2009).
7. Titanium Nickelide Alloys Having Shape Memory. Part I. Structure, Phase Transformations, and Properties [in Russian], Publishing House of the Ural Branch of the Russian Academy of Sciences, Ekaterinburg (2006).
8. V. N. Khachin, S. A. Muslov, V. G. Pushin, and V. V. Kondrat'ev, Metallofizika, **10**, No. 1, 102–104 (1988).
9. V. G. Pushin, V. V. Kondrat'ev, and V. N. Khachin, Pretransitive Phenomena and Martensitic Transformations [in Russian], Publishing House of the Ural Branch of the Russian Academy of Sciences, Ekaterinburg (1998).
10. O. Mercier, K. N. Melton, G. Gremand, and J. Hagi, J. Appl. Phys., **51**, No. 3, 1833–1834 (1980).
11. M. P. Kashchenko, I. V. Aleksina, V. V. Letuchev, and A. V. Nefedov, Fiz. Met. Metalloved., **80**, No. 6, 10–15 (1995).
12. V. V. Letuchev, V. P. Vereshchagin, and M. P. Kashchenko, J. Physique IV, **5**, No. C8, C8-151 (1995).
13. T. Sabury, J. Watanabe, and S. Nenno, ISIJ International, **29**, No. 5, 405–411 (1989).
14. M. P. Kashchenko and V. G. Chashchina, Dynamic Model of Formation of Twinned Martensite Crystals during γ-α Transformation into Iron Alloys [in Russian], Publishing House of Ural State Forest Engineering University, Ekaterinburg (2009).
15. M. Kashchenko and V. Chashchina, Dynamic Theory of γ-α Martensitic Transformation in Iron-Based Alloys. Solving the Problem of the Formation of Twinned Martensite Crystals, LAMBERT Academic Publishing, Saarbrucken, Germany (2012).